Sensors & Actuators: B. Chemical 409 (2024) 135578

Contents lists available at ScienceDirect

Sensors and Actuators: B. Chemical

journal homepage: www.elsevier.com/locate/snb

Breath analysis system with convolutional neural network (CNN) for early detection of lung cancer

Byeongju Lee [a,b], Junyeong Lee [a], Jin-Oh Lee [a], Yoohwa Hwang [c], Hyung-Keun Bahn [c], Inkyu Park [b], Sanghoon Jheon [c,*], Dae-Sik Lee [a,*]

[a] Electronics and Telecommunications Research Institute (ETRI), Daejeon 34129, Republic of Korea
[b] Korea Advanced Institute of Science and Technology, Daejeon 34141, Republic of Korea
[c] Seoul National University Bundang Hospital, Seoul 13620, Republic of Korea

ARTICLE INFO

Keywords:
Lung cancer
Exhaled breath
Breath analyzer
Multimodal sensor array
Convolutional neural network (CNN)

ABSTRACT

Early diagnosis of lung cancer, the leading cause of cancer-related death worldwide, is critical for reducing mortality rate. However, current diagnostic methods are invasive, time-consuming, costly, and may not always provide accurate diagnoses. For early diagnosis, recent research has focused on noninvasive approaches, including the detection of volatile organic compounds (VOCs) in human exhaled breath. Changes in the composition and concentration of VOCs in exhaled breath may indicate lung cancer, and this approach offers several advantages over traditional diagnostic methods. Moreover, the combination of a breath gas sensing system and machine learning algorithms provides a more accurate diagnosis. In this study, for the early diagnosis of lung cancer, a breath analysis system was developed using a gas sensor array and deep learning algorithm. The breath analysis system was designed to detect multiple VOCs in exhaled breath using ten semiconductor metal oxide (SMO), one photoionization detector (PID), nine electrochemical (EC) gas sensors. In total, 181 clinical breath samples (from 74 healthy controls and 107 lung cancer patients) were collected and analyzed using a 1D convolutional neural network (CNN) algorithm. The results showed an overall accuracy of 97.8% in classifying healthy controls and lung cancer patients using a complete clinical dataset. Through a comparison of the single-sensor type data and multimodal sensor data and performance analysis of three different deep learning models (multilayer perceptron, recurrent neural network, and CNN), we validated the potential of the breath analyzer with a multimodal sensor system and a 1D CNN as a lung cancer diagnostic device.

1. Introduction

Lung cancer is a serious and lethal disease that poses significant global health challenge. According to the recent study, the incidence rate of lung cancer is 11.4%, making it the second most common cancer after breast cancer [1]. In addition, lung cancer has been identified as the leading cause of cancer-related deaths, with an estimated 1.8 million deaths. Its severity lies not only in its high incidence but also in that it is frequently diagnosed at advanced stages, leading to limited treatment options. In 2014, the UK Office for National Statistics reported a 1-year survival rate for stages I and IV patients at 85% and less than 20%, respectively [2]. Therefore, early diagnosis is crucial for reducing the mortality rate of lung cancer. As a leading cause of cancer-related mortality worldwide, lung cancer requires continuous research to improve early diagnosis.

Current diagnostic methods for lung cancer, including chest X-ray (CXR), computed tomography (CT), bronchoscopy, and liquid biopsies are invasive, expensive, time-consuming, and inaccurate [3–5]. False positives and an inability to distinguish between benign and malignant lesions can lead to unnecessary invasive procedures and patient anxiety [6]. Exhaled breath analysis, which utilizes sensitive breath sensors, is a promising method for enhancing the diagnosis of lung cancer [7–9]. Volatile organic compounds (VOCs) are present in exhaled breath, and their composition and concentration vary based on organ malfunction. Breath sensors detect changes in VOCs in exhaled breath, thereby diagnosing specific diseases. This non-invasive and rapid method offers great potential for detecting biomarkers suggestive of early stages of lung cancer.

Through the analysis of VOC patterns, researchers have aimed to develop highly accurate and cost-effective diagnostic devices. The

* Corresponding authors.
E-mail addresses: jheon@snu.ac.kr (S. Jheon), dslee@etri.re.kr (D.-S. Lee).

https://doi.org/10.1016/j.snb.2024.135578
Received 30 October 2023; Received in revised form 14 February 2024; Accepted 29 February 2024
Available online 2 March 2024

Table 1
Clinical characteristics of the participants.

	Lung cancer (n = 90)		Healthy control (n = 74)		*p* value	
Sex	Male	54 (60%)	Male	43 (58.1%)	0.775	
	Female	36 (40%)	Female	31 (41.9%)		Female
Age (years)		68.6 ± 8.5		51.1 ± 16.9	< 0.001	
Histology	Small cell lung cancer	1 (1.1%)				
	Adenocarcinoma	63 (70%)				
	Squamous	19 (21.1%)				
	Other	7 (7.8%)				
Stage	IA	35 (38.9%)				
	IB	10 (11.1%)				
	IIA	10 (11.1%)				
	IIB	8 (8.9%)				
	IIIA	15 (16.7%)				
	IIIB	1 (1.1%)				
	IV	11 (12.2%)				

analysis of exhaled breath VOCs using gas chromatography-mass spectrometry (GC-MS) has been widely reported [10–12]. GC-MS can accurately detect various VOCs; however, it is expensive, time-consuming, and requires specialized expertise [13]. Furthermore, exhaled breath contains numerous VOCs in extremely small amounts, and the differences in VOC concentrations between healthy individuals and lung cancer patients often do not exhibit significant variations at the parts per billion (ppb) level [14,15]. To address these challenges, research has predominantly focused on developing electronic nose (E-nose) systems using multiple gas sensors and conducting a pattern analysis of the responses from these sensors to diagnose lung cancer. In previous studies, colorimetric [16], surface acoustic wave (SAW) [17], carbon-polymer array [18], quartz microbalance (QMB) [19], carbon nanotube-based [20], electrochemical (EC) [21], and semiconductor metal oxide (SMO) gas sensors [22] were utilized as breath analyzers. Each sensor exhibits unique characteristics and acquires distinct patterns from exhaled breath. Therefore, a multimodal gas-sensor system utilizing various types of sensors can capture a more extensive range of pattern information than a single-type sensor system [23–26]. In this study, we utilized three types of gas sensors–SMO, EC, and photoionization detector (PID)–to acquire diverse exhaled-breath patterns.

Additionally, various methods for analyzing the patterns obtained using breath analyzers have been studied extensively. The data obtained using the sensor array were used to classify lung cancer patients using learning models such as support vector machine (SVM) [26], linear discriminant analysis (LDA) [27], backpropagation neural network (BPANN) [28], k-near neighbor (k-NN) [29], and logistic regression analysis (LRA) [30]. Previously, our research team developed a breath analyzer with a multilayer perceptron (MLP) for lung cancer diagnosis [5]. While the analysis of VOC patterns in exhaled breath showed potential for early diagnosis of lung cancer, its practical application was limited owing to its relatively low diagnostic performance and requirement of feature data extraction. Among the various deep-learning models, 1- dimension convolutional neural networks (1D CNNs) have proven to be effective in capturing patterns in time-series data, making them suitable for various applications, including natural language processing, sensor data analysis, and financial time-series forecasting [31]. Furthermore, several studies have reported the use of 1D CNNs for diagnosing diseases by analyzing time-series data [32,33].

In this study, we explored the convergence of a breath analyzer with a multimodal gas sensor array and 1D CNN for the early diagnosis of lung cancer. The breath analyzer consisted of three types of gas sensors, valves, a mass flow controller (MFC), desorption tube, and lamp. The system was designed to enable automatic data collection using a gas flow control module. The multimodal sensor system can extract a wider range of patterns from exhaled breath data than a single-type sensor array, and the collected breath data are classified using the 1D CNN model. A total of 181 breath samples, from 74 healthy individuals and 107 lung cancer patients, were used in the application of 1D CNN. To validate the performance of the multimodal sensor system and 1D CNN model used in this study, we compared its classification performance with that of single-type sensor data and different deep learning models.

2. Experimental procedures

2.1. . Study population

We enrolled 164 participants (90 lung cancer patients and 74 healthy individuals) voluntarily at Seoul National University Bundang Hospital. The healthy control group consisted of individuals aged >18 years who were not receiving treatment for any respiratory conditions. Lung cancer patients were selected based on the following criteria: histological confirmation of the primary or metastatic site, presence of intrabronchial lesions, central lesions within the inner one-third of the hilum on chest CT, or peripheral lesions located beyond the outer one-third of the pulmonary hilum with tumors measuring >2 cm on chest CT. Lung cancer patients who had metabolic diseases and respiratory system disorders, such as chronic obstructive pulmonary disease (COPD) and pneumonia, were excluded from the study. Clinical characteristics of the enrolled participants are summarized in Table 1.

2.2. . Design and fabrication of the breath analyzer with multimodal sensor array

To design the optimal chamber shape that can facilitate a uniform gas measurement environment, we performed numerical simulations using the COMSOL Multiphysics. The dimensions of the sensors, based on the commercial electrochemical sensor SS2198 (SENKO, Korea), were reflected as a diameter of 2 cm and a height of 2 cm, including the electrode. In this simulation, two types of gases (buffer gas and sample gas) were employed. N_2 was chosen as the buffer gas due to its chemical stability, being one of the most commonly used carrier gases. Additionally, acetone, known for its easy generation during body metabolism, was selected as the sample gas. Throughout the simulation process, the chamber's interior was initially purged with N_2 at 1 atm. The flow rate of the sample gas, acetone, entering the chamber was set to 500 sccm, with a concentration of 1 mol/m^3.

A multimodal sensor system consists of three types of gas sensors: SMO, EC, and PID. Each method offers unique advantages for the detection of VOC markers. First, the SMO gas sensor provides stable gas measurements with a fast response speed and high sensitivity [34]. Furthermore, it allows the development of various gas sensors by modifying the composition of the sensing material, thereby enabling easy customization of gas selectivity. By utilizing multiple types of SMO gas sensors, multiple output analyses can be performed to overcome the challenge of low selectivity resulting from the cross-sensitivity observed in individual gas sensors. The SMO gas sensors used in the system included TGS2444, TGS2600, TGS2602, TGS2603, TGS2610, TGS2611,

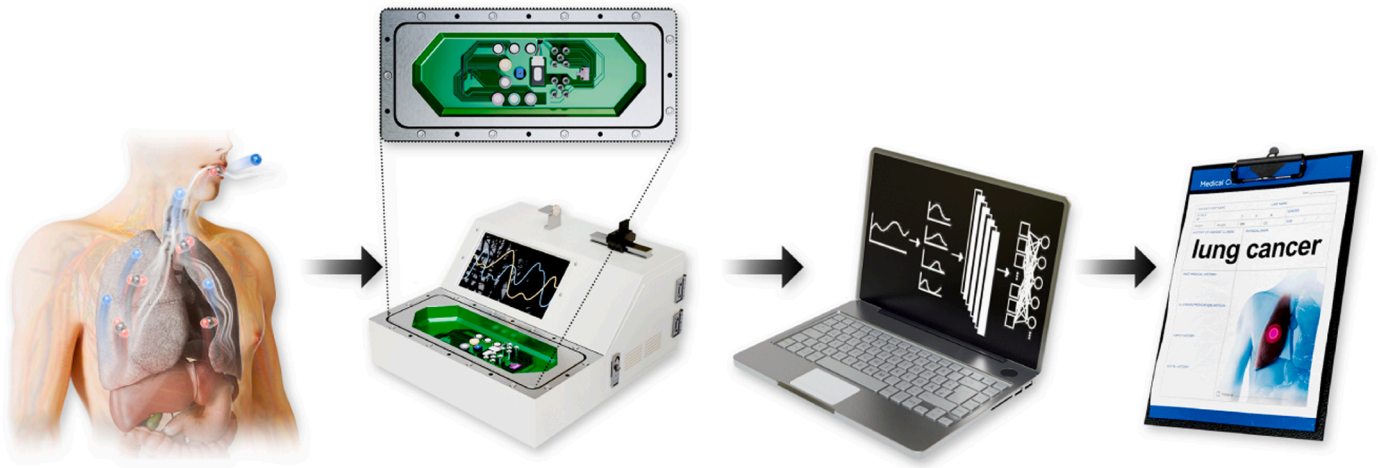

Fig. 1. Schematic diagram of the breath analyzer and strategy for lung cancer diagnosis.

TGS2612, TGS2620, and TGS3870 from Figaro (Japan) and RSM741 from RNSLab (Korea). Secondly, EC gas sensors operate at low power, offering high sensitivity, and a wide measurement range [35]. This method facilitated the detection of promising VOC marker candidates. The EC gas sensors SS21F8, SS2128, and SS2198 from SENKO (Korea) and NE4HCHO, NE4H2S, NE4NH3, NE4NO2, NE4CO, and NE4NO from Nemoto (Japan) were utilized in this system. Finally, the PID gas sensor demonstrated the highest selectivity compared to the other methods, making it suitable for detecting ultra-trace VOC markers [36]. We utilized miniPID2 (ION Science, UK) as the PID gas sensor. We implemented a multimodal gas sensor array by employing 20 types of advanced gas sensors, leveraging their strengths and compensating for their weaknesses using different measurement methods. The results comparing the response of MOS gas sensors and PID gas sensors to different gases are presented in fig. S2. Electrochemical gas sensors, which are susceptible to damage due to high sensitivity to specific gases, were excluded from this response comparison test.

2.3. . Exhaled breath sampling process

We collected exhaled breath samples from two groups: lung cancer patients (LC, experimental group) and healthy controls (HC, control group). We validated the developed multimodal gas sensor system by measuring 107 LC and 74 HC samples. To ensure consistency in the collection process, the following steps were followed.

a) Pretreatment (exhalation gas collection 1 day prior): Participants were instructed to adhere to dietary restrictions, limit alcohol, and consume strongly seasoned meals. They fasted for at least 4 hours before the examination. b) Exhaled gas collection: Participants refrained from brushing their teeth within 2 hours before exhaling into the collection device. They performed deep breathing at least five times before sample collection and rinsed their mouths with sterilized distilled water. A total volume of 3 L exhaled air was collected in a Tedlar bag. c) Adsorption of samples in Tenax tube: We adsorbed the collected breath samples onto a Tenax tube within 2 hours of collection, with an adsorption rate of 0.1 L/min.

Subsequently, an exhaled breath sample adsorbed onto a Tenax tube was inserted into the developed system. We then measured the desorbed exhaled breath samples from the Tenax tube using the multimodal sensor system. The Tenax tube, integrated into the system, is heated to 280℃ for the desorption of the adsorbed exhaled air sample. The exhaled breath sample, desorbed through tube heating, is then transported to the gas chamber by the carrier gas (dry N_2). During this transfer, the heated exhaled breath sample is cooled by the carrier gas of room temperature. The gas sample within the chamber is maintained at a temperature of approximately 40℃ and a relative humidity of 0. We conducted measurements on the desorbed exhaled breath samples moving into the chamber using the developed multimodal gas sensor array module.

2.4. . Data analysis

In the sensor data analysis, the responses of the 19 sensors were defined by dividing the sensor values throughout the entire measurement period (R_{breath}) by the sensor values just before the VOCs were desorbed from the Tenax tube (R_{air}), which served as the reference point. The gas sensor responses were analyzed by grouping sensors with similar reactivity, considering the data separately for SMO, EC, and PID gas sensors.

Breath response data were utilized in neural networks for pattern analysis and employed to classify healthy controls and lung cancer patients. First, the classification performance of lung cancer patients using the 1D CNN model was evaluated. Next, we investigated the effectiveness of the multimodal sensor system applied to the breath analyzer by comparing the single-type sensor and entire sensor data. The classification performance of the models was analyzed by comparing accuracy, sensitivity, and specificity, calculated using the following equations, respectively.

$$\text{Accuracy}(\%) = \frac{\text{TP} + \text{TN}}{\text{TP} + \text{FN} + \text{TN} + \text{FP}} \times 100$$

$$\text{Sensitivity}(\%) = \frac{\text{TP}}{\text{TP} + \text{FN}} \times 100$$

$$\text{Specificity}(\%) = \frac{\text{TN}}{\text{TN} + \text{FP}} \times 100$$

where TP is true positive; FP, false positive; TN, true negative; and FN, false negative

Finally, the classification performance of the 1D CNN model was compared with that of the MLP and recurrent neural network (RNN) models. In the analysis of these models, by including the parameters mentioned above, we evaluated the performance of the model using receiver operating characteristic (ROC) curves. The ROC curve illustrates the relationship between sensitivity and specificity under a specific boundary condition, and the area under the curve (AUC) values served as the evaluation metric for the model's performance in classifying lung cancer patients and healthy controls.

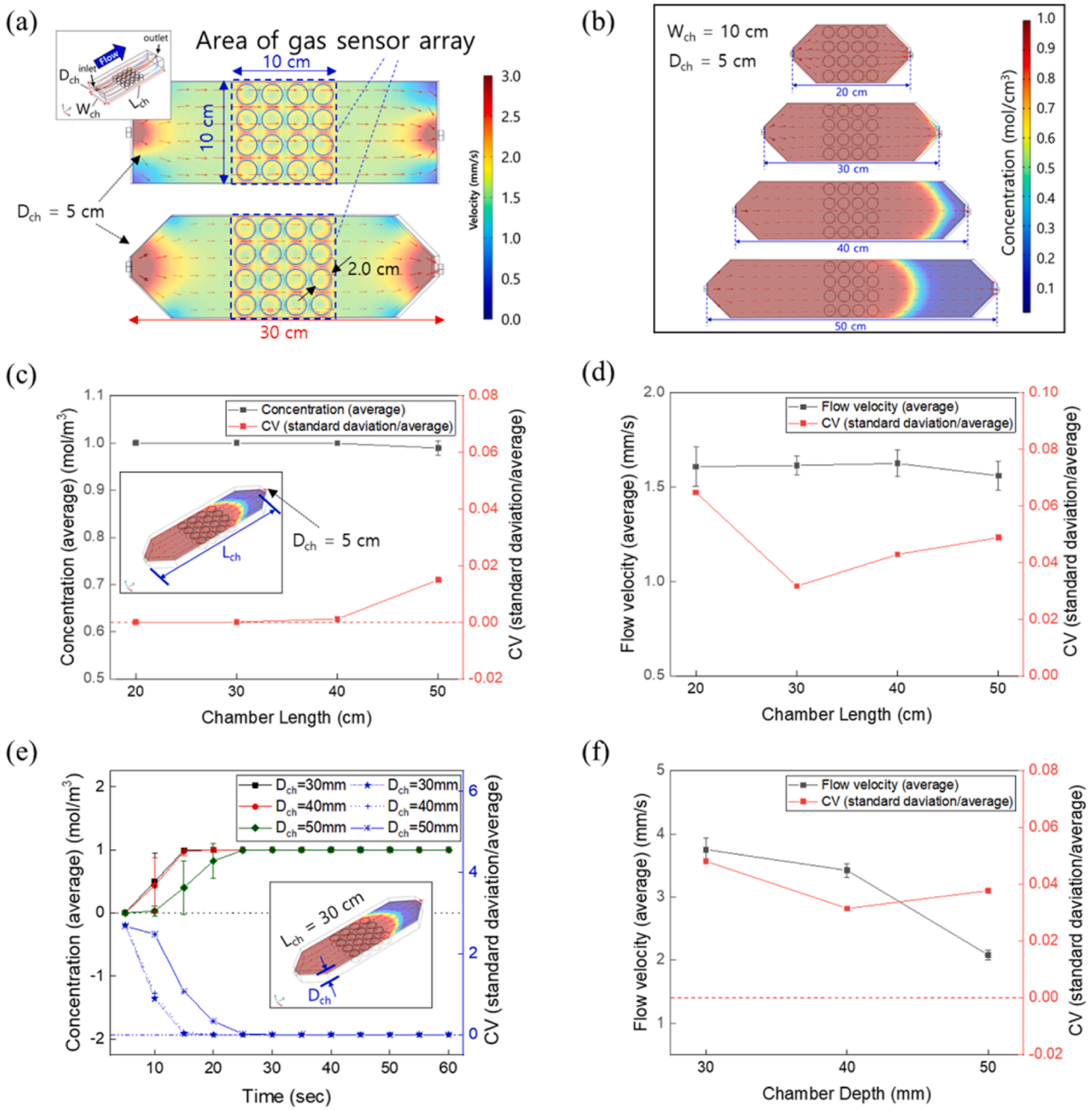

Fig. 2. Simulation results for optimal chamber design. (a) Fluid velocity distribution at various locations within the chamber based on chamber edge shapes. A significant decrease in dead volume area is observed in the lower chamber compared to the upper chamber. (b) Simulation results of fluid velocity and gas concentration for each channel length (Lch) after 60 seconds of gas injection. (c) Graphs depicting the mean and CV of concentration at each gas sensor's center for different Lch values. The mean and CV remain highly stable for Lch = 20–40 cm. (d) Graphs representing the mean and CV of velocity at each gas sensor's center for different Lch values. The mean velocity remains nearly the same across the four conditions, with the lowest CV observed at Lch = 30 cm. (e) Graphs displaying the mean and CV of concentration at each gas sensor's center with respect to Dch and gas inflow time. From 30 seconds onwards, highly stable results are observed for all conditions, irrespective of Dch. (f) Graphs showing the mean and CV of velocity at each gas sensor's center for different Dch values. The lowest CV value is observed at Dch = 40 mm.

3. Results and discussion

3.1. Fabricated breath analyzer with multimodal sensor system

Fig. 1 shows the schematic diagram of the breath analysis system and strategy for lung cancer diagnosis. When exhaled breath samples collected from both healthy controls and lung cancer patients were injected into the breath analyzer, the sensor array data were measured using an automated system. The measured exhaled breath data were used to diagnose lung cancer using a deep-neural-network-based classification model. The feasibility of using a multimodal sensor system with three types of gas sensors and training it with time-series data using a 1D CNN was evaluated to validate its potential as a practical lung cancer diagnostic device.

The structure of the gas sensor chamber and arrangement of the sensors were designed to optimize the gas flow based on the results of the gas flow simulation, as shown in Fig. 2. Firstly, an analysis of the dead volume within two types of chambers was conducted to identify a

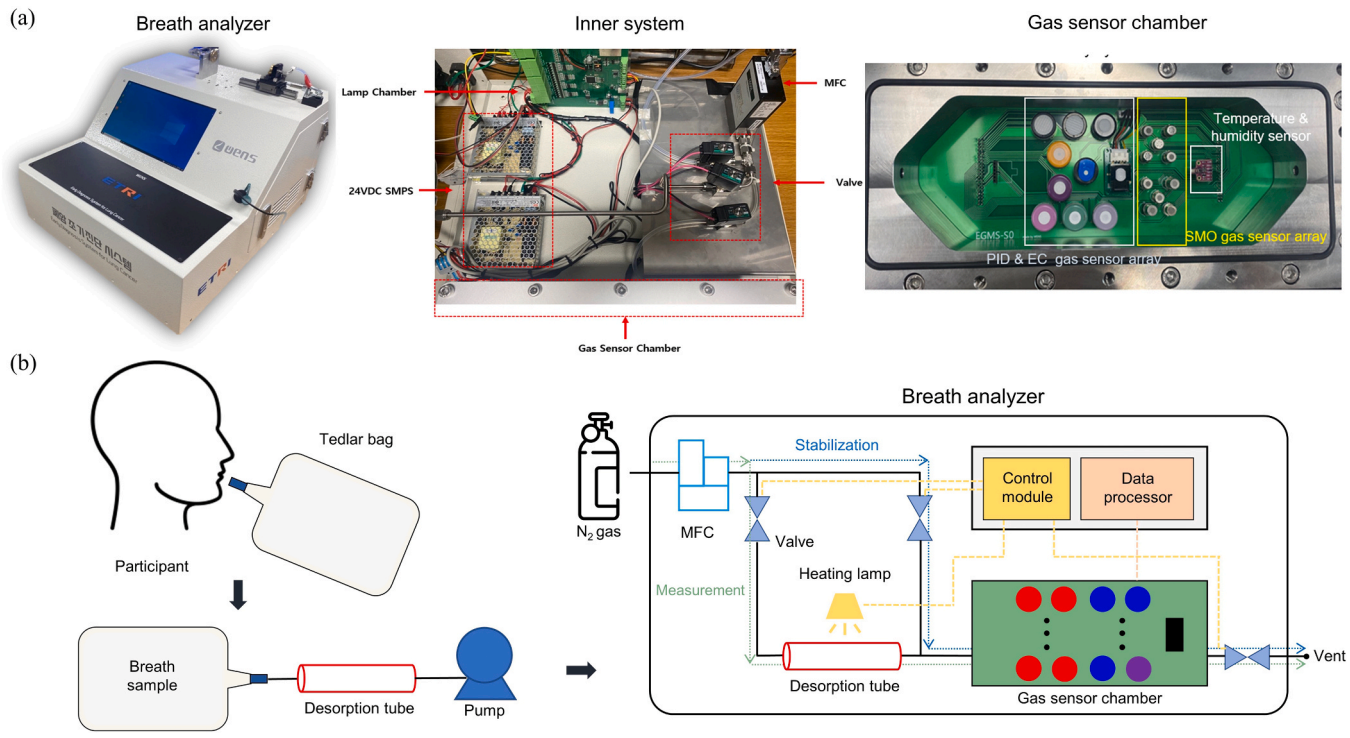

Fig. 3. Description of the breath analyzer with multimodal sensor array and its operation. (a) Real images of the breath analyzer and its inner systems. (b) Diagram of operation process of the breath analyzer.

chamber structure that can facilitate a uniform gas concentration and flow environment throughout the entire chamber. The upper part of Fig. 2(a) presents the simulation results of fluid flow within the most common rectangular chamber shape. This simulation revealed dead volumes, accounting for less than half the flow velocity compared to the sensor area, at the four corner regions. Such dead volumes not only hinder the fluid flow within the chamber but also lead to issues such as residue from previous sample gases during chamber cleaning for different sample measurements. To address this, we designed a chamber with edges cut at a 45° angle and conducted the same simulation. The simulation demonstrated a reduction of over 80% in the chamber's dead volume. Secondly, to determine the optimal channel length (Lch, the width of the chamber), an analysis of fluid velocity and gas concentration at each sensor's center in the sensor area was conducted for Lch values of 20, 30, 40, and 50 cm. Fig. 2(b) illustrates the gas concentration distribution (colormap) and flow velocity (red arrow) within the chamber after 60 seconds of gas injection under each condition. The gas concentration and flow velocity at the sensor area appear to be uniform in each chamber. For a precise comparison of concentration and velocity uniformity across different Lch values, we analyzed the concentration and velocity at each of the 16 sensors. Fig. 2(c)-(d) represent graphs depicting the average and Coefficient of Variation (CV, standard deviation/average) of concentration and flow velocity at the centers of the sensors for each Lch value. Initially, the average concentration values show independence with respect to Lch, but the CV values of the concentration significantly increase by over tenfold at 50 cm (0.015 AU) compared to other Lch values (~ 0 AU). Similarly, for velocity, while the mean values show almost no dependence on Lch, the smallest CV is observed at Lch = 30 cm. Table S1 shows the individual gas concentration and flow velocity data at each sensor position. Thirdly, to determine the optimal channel depth (Dch, the height of the chamber), an analysis of fluid velocity and gas concentration at each sensor's center in the sensor area was conducted for Dch values of 3, 4, and 5 cm. As evident in Fig. 2(e), the average and CV values of the concentration for Dch = 3 and 4 cm are nearly identical. However, for velocity, the lowest CV value is observed at Dch = 4 cm in the graph presented in Fig. 2(f). Table S2 presents the raw data corresponding to the graphs in Figs. 2(e)–2(f). Through simulations, we determined the optimal chamber design as Lch: Wch: Dch = 30 cm: 10 cm: 4 cm and the chamber shape.

Fig. 3 shows real images of the breath analyzer and details of the operational process for breath data collection. Fig. 3(a) shows the breath analyzer, inner components, and gas sensor chamber with a multimodal sensor array. The breath analyzer consisted of valves, an MFC, a 24VDC switching mode power supply, a lamp for gas flow control, and gas sensor chamber for measurement. The gas sensor chamber was composed of SMO, EC, PID, and temperature/humidity sensors. Fig. 3(b) illustrates the process from exhaled breath collection to tube adsorption, breath-sample measurements, and chamber cleaning. The process was divided into two stages: exhaled-breath sample collection and sample measurement. First, the participants' exhaled breath was collected in a Tedlar bag. To adsorb the VOCs within the collected breath sample, a pump was used to draw the sample into a Tenax tube. The VOCs adsorbed in the Tenax tube were measured using the multimodal sensor system of the breath analyzer. The measurement system was automated and the control module regulated the valves, MFC, and heating lamp within the breath analyzer. The total breath data collection process took 40 min, which included the stabilization and measurement processes. Before measuring the exhaled breath sample, the gas-sensor chamber was stabilized in a nitrogen atmosphere for 15 min (blue dotted line). Then, the gas adsorbed in the Tenax tube was desorbed by heating it to 300°C, and measured over 25 min (green dotted line). The sensor response data can be viewed in real-time on a monitor and automatically saved on a personal computer.

3.2. Sensor characteristics of exhaled breath samples

Prior to deep learning-based classification, we analyzed the acquired sensor response data from healthy individuals and lung cancer patients. Fig. 4 shows the response of the gas sensor array to the collected exhaled breath. The graphs show the responses of the 19 gas sensors, excluding the TGS3870 gas sensor, owing to its relatively unstable response data.

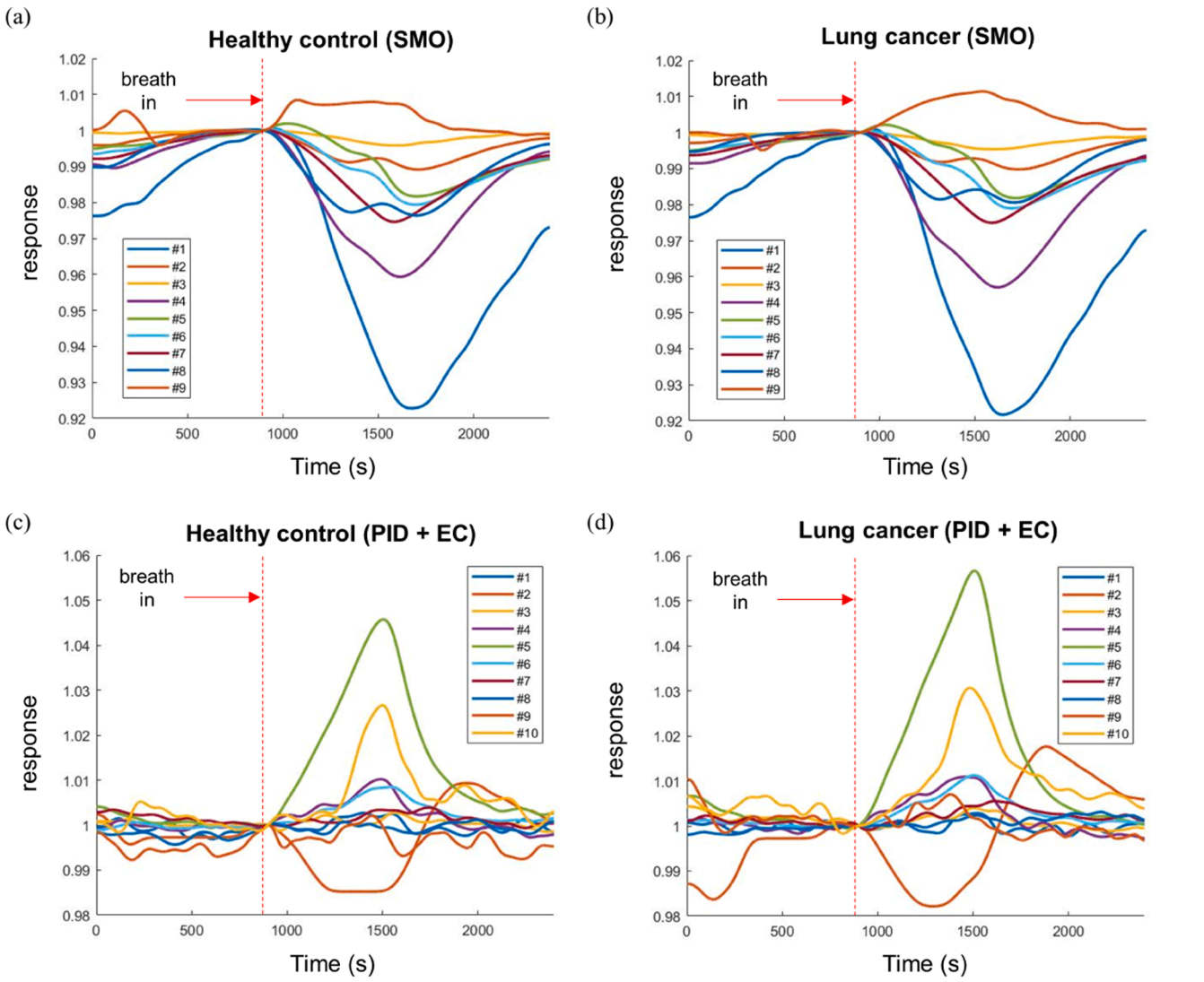

Fig. 4. Response of the SMO sensors to the exhaled breath from (a) a healthy control and (b) a lung cancer patient. Response of the PID and EC sensors to the exhaled breath from (c) a healthy control and (d) a lung cancer patient.

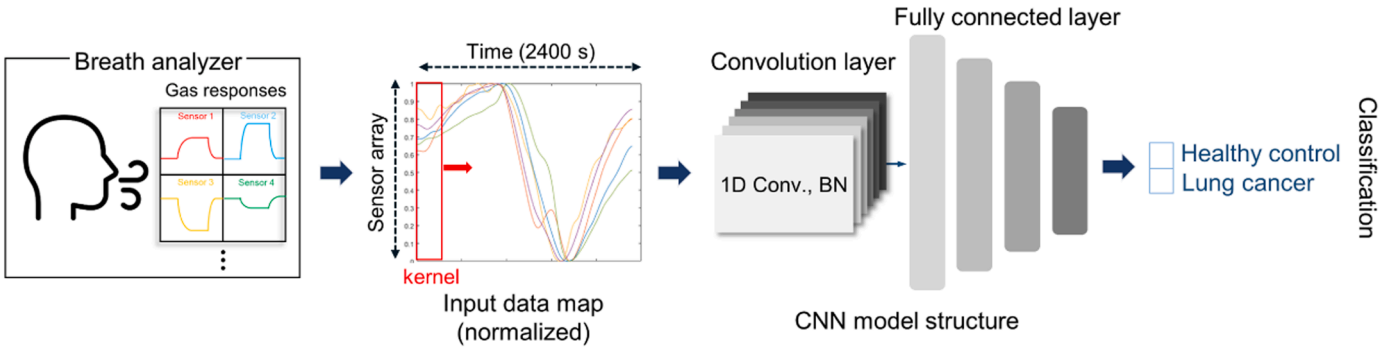

Fig. 5. Structure of breath analyzer and convolutional neural network (CNN) algorithm for lung cancer diagnosis.

The detailed labels of the 19 gas sensors are listed in Table S3. Each sensor exhibited different sensitivities and response times. Specific sensors (i.e., SMO #2, PID + EC #5, and PID + EC #10) showed a higher response to the exhaled breath of a patient with lung cancer. The SMO sensors exhibited a peak at approximately 700 s after the introduction of the exhaled breath, whereas the PID and EC sensors showed a peak at approximately 600 s. Differences in response and response times occurred because each gas sensor reacted differently to various VOCs, which they are specifically designed to detect. This diversity in sensor reactions enhances the availability of information for lung cancer diagnosis.

Table 2
Key parameters of breath analyzer using 5-fold cross-validation of 1D-CNN for all breath samples.

		Pathology HC (negative)	LC (positive)	Total	Sensitivity (95% CI)	Specificity (95% CI)	AUC (95% CI)
Breath analyzer	HC (negative)	71.2	1.2	72.4	98.9% (98.2%~ 99.6%)	96.2% (95.2%~ 97.2%)	97.8% (97.3%~ 98.3%)
	LC (positive)	2.8	105.8	108.6			
	Total	74	107	181			

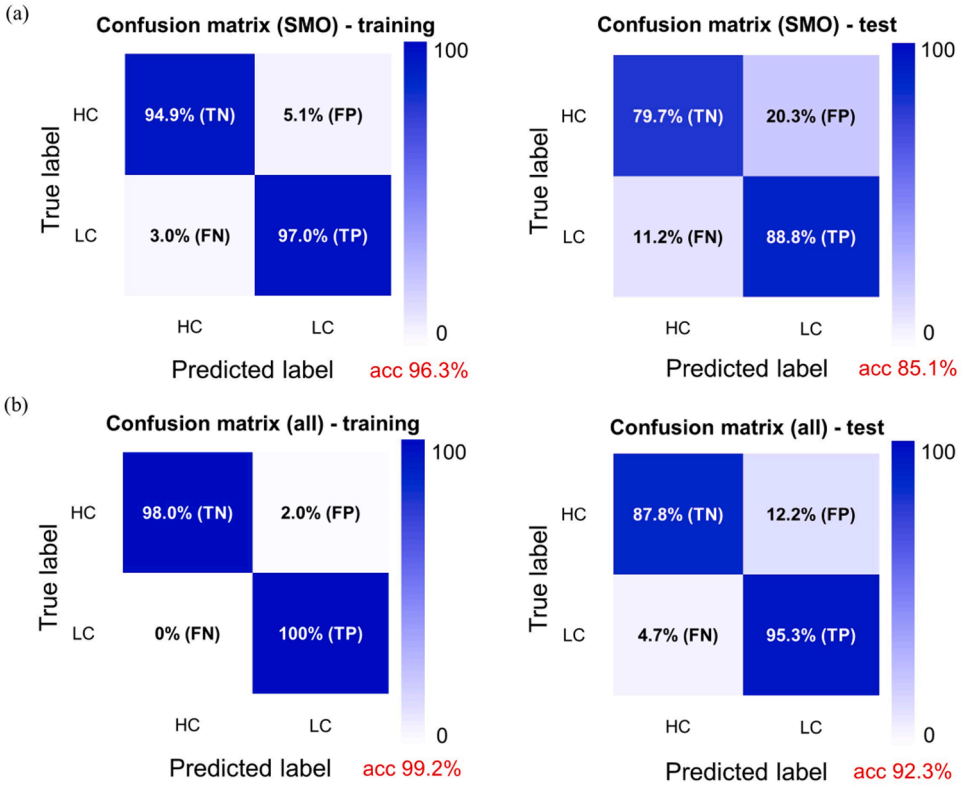

Fig. 6. Lung cancer diagnosis results with different sensor array data. (a) SMO gas sensor array, and (b) multimodal sensor array.

3.3. Breath analyzer performance in lung cancer diagnosis

A 1D CNN was adopted to classify lung cancer patients using multimodal sensor array data. The model was built utilizing an open-source library (PyTorch, Meta, USA). The training and evaluation of 1D CNN were carried out in a high-performance computing environment utilizing a GPU (RTX Titan, NVIDIA, USA). Fig. 5 shows the structure of a 1D CNN used in lung cancer diagnosis. To reduce bias during the training process, breath-response data were normalized to a range between 0 and 1 using the following equation, where R_{max} is the maximum and R_{min} is the minimum response:

$$R_{nor} = (R\text{-}R_{min}) / (R_{max}\text{-}R_{min})$$

The normalized response data were fed into the 1D CNN model in a 19×2400 matrix, where 19 was the number of multimodal gas sensors and 2400 was the total measurement time during breath collection. A 1D CNN consists of a convolutional layer and a fully connected layer. In the convolutional layer, six kernels were used for the convolutional operation and were configured to move only along the time axis to construct a 1D CNN model. The classification was then conducted using three fully connected layers. Each convolutional and fully connected layer used a rectified linear unit (Leaky-Relu) as the activation function and batch normalization layer. The last layer outputs two nodes with the lung cancer diagnosis results. This layer employed the softmax function as its activation function to calculate the probability of being a patient with lung cancer.

In some cases, multiple breath samples were obtained from lung cancer patients, resulting in 181 breath samples, including 74 and 107 breath samples from healthy controls and lung cancer patients, respectively, which were used as input data for deep learning. The datasets were randomly divided into the following two groups: 80% and 20% of the data were used for training and testing, respectively. The deep learning models were trained using the training dataset, and their performance was evaluated using the test dataset. In this study, 5-fold cross-validation was applied to prevent overfitting, and the classification performances were averaged across the cross-validation folds. Table 2 summarizes the classification results of the clinical breath samples collected using the 1D CNN breath analyzer model. When the entire dataset was evaluated by 5-fold cross-validation, it exhibited a sensitivity of 98.9%, specificity of 96.2%, and AUC of 97.8%. These results demonstrate a remarkably high classification accuracy, validating the reliability of the 1D CNN model for lung cancer diagnosis.

We conducted additional analysis for the classification of lung cancer stages. The lung cancer patient group was divided into early stages (I+II) and advanced stages (III+IV) and applied a 1D CNN model for classification. The classification results for early-stage and advanced-stage lung

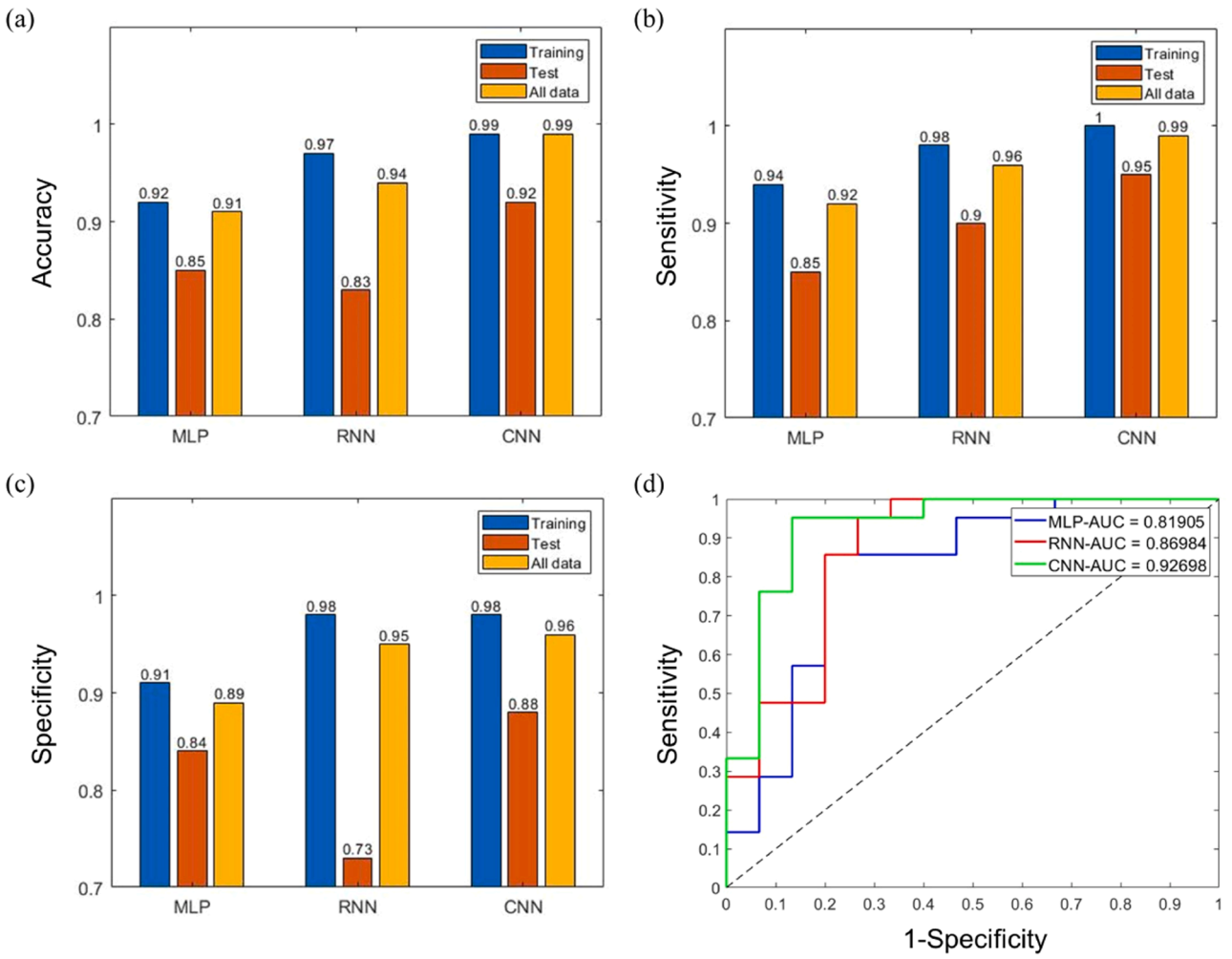

Fig. 7. Comparison of classification performance in different deep learning models (MLP, RNN, and CNN). (a) Overall accuracy, (b) sensitivity, (c) specificity of training, validation, and test datasets from three different deep learning algorithms. (d) Receiver operating characteristics (ROC) curves and AUC values of the test datasets. All values are the averages of the results from 5-fold cross-validation.

Table 3
Comparison of the lung cancer diagnosis results between previous studies using breath sensor system and this study.

Ref	Number of breath samples	Sensor array type	Classification algorithm	Accuracy	Sensitivity	Specificity
Chang et al. [5]	85 breath samples (48 HC + 37 LC)	7 SMO gas sensor	MLP	75.0	79.0	72.0
Goor et al. [22]	46 breath samples (107 HC + 60 LC)	Aeonoses (3 SMO gas sensor)	ANN	86	88	86
Gasparri et al. [19]	146 breath samples (76 HC + 70 LC)	8 quartz microbalance (QMB)	PLS-DA	-	81	91
Tirzite et al. [37]	244 breath samples (79 HC + 165 LC)	Cyranose 320 (32 polymer carbon black composite gas sensor)	SVM	-	98.8	81.0
Shlomi et al. [23]	46 breath samples (16 HC + 30 LC)	Multimodal gas sensor (26 gold nanoparticle + 8 SWCNT/PAH + 6 SWNCT/HBC sensor)	DFA	87.0	75.0	93.3
Li et al. [24]	52 breath samples (28 HC + 24 LC)	Multimodal gas sensor (8 SMO + 1 catalytic combustion + 1 hot-wire + 4 EC gas sensor)	LDA-Fuzzy-5-NN	91.6	91.6	91.7
Liu et al. [25]	82 breath samples (36 HC + 46 LC)	Multimodal gas sensor (12 SMO + 1 hot-wire + 1 solid electrolyte + 5 EC gas sensor)	SVM + SGL	94.3	97.8	90.2
Chen et al. [26]	235 breath samples (134 HC + 101 LC)	Multimodal gas sensor (2 EC + 1 hot-wire + 1 catalytic combustion + 7 SMO gas sensor)	KPC + XGBoost	93.6	95.6	91.1
This work	181 breath samples (74 HC + 107 LC)	Multimodal gas sensor (10 SMO + 1 PID + 9 EC gas sensor)	1D CNN	97.8	98.9	96.2

cancer are presented in Table S4. In this experiment, each patient contributed only one breath sample, with 63 breath samples for early-stage and 27 samples for advanced-stage. The classification results are presented in Table S4. Early-stage and advanced-stage lung cancer patients were distinguished with an accuracy of 80.9%.

Fig. 6 shows the classification performance of the model with changes in the dataset. Datasets using only the SMO gas sensor array and those using all the gas sensor arrays (SMO, EC, and PID) were used to train separate 1D CNN models. When using only SMO gas sensor data, the model achieved an accuracy of 96.3% during training and 85.1% during testing. However, it exhibits an accuracy of 99.2% during training and 92.3% during testing when the entire sensor data was used. In particular, the specificity of the training dataset was significantly improved, leading to an overall improvement in the classification performance of the test set. These results validate that using several patterns obtained from multimodal sensors as dataset achieves a higher classification accuracy than using patterns obtained from a single sensor type.

Fig. 7 shows the classification performance of the different deep learning algorithms. For comparison, we selected the three most commonly used deep-learning algorithms: the MLP, RNN, and CNN. The hyperparameters of the three algorithms were optimized to achieve the best classification performance. Fig. 7(a)–(c) show the accuracy, sensitivity, and specificity of the training, test, and all datasets, respectively, for the three deep learning algorithms. All three algorithms exhibited high accuracy with the training dataset; however, the MLP and RNN exhibited relatively lower accuracy with the test dataset. The MLP model had a lower overall classification accuracy compared to other models, while the RNN model exhibited overfitting tendencies towards lung cancer patients. The 1D CNN model exhibited the most similar accuracy, sensitivity, and specificity between the training and test datasets, indicating that it was the most reliable algorithm. Next, we analyzed the performance of the three deep learning algorithms using ROC curves and their AUC values. The CNN model had the highest AUC value (92.7%), followed by the RNN (87.0%) and MLP (81.9%).

Table 3 shows the breath analyzers and their classification performances in previous studies and this study. Conventional studies utilizing single-type sensor arrays for lung cancer diagnosis have shown a relatively lower classification performance. Recent studies employing multimodal sensor systems have demonstrated improved accuracy using data from various types of gas sensors. Previous studies utilized feature extraction methods for data preprocessing [13,14,26], whereas in this study, the use of the 1D CNN model allowed for the omission of such a feature extraction process. Furthermore, we achieved an accuracy of 97.8%, sensitivity of 98.9%, and specificity of 96.2% for lung cancer diagnosis. Compared to other breath sensor systems, our breath analyzer demonstrated a significant capability to effectively distinguish between lung cancer patients and healthy individuals.

4. Conclusions

We fabricated a breath analyzer with a multimodal gas sensor array and analyzed it using a deep learning algorithm for the early diagnosis of lung cancer. The breath analyzer consisted of three types of gas sensor arrays and highly automated systems including a flow control module, heating lamp, MFC, and valves. A multimodal sensor system composed of SMO, EC, and PID gas sensors can capture various exhaled breath patterns, which are recognized using a 1D CNN-based classification model. Using the breath analyzer, we collected 181 breath samples (74 healthy controls and 107 lung cancer patients) and successfully distinguished between the two groups with a high accuracy of 97.8% using a 1D CNN algorithm. Furthermore, the validity of the multimodal sensor array and 1D CNN model used in this study was confirmed by comparing its classification performance with that of single-sensor system data and other deep-learning algorithms, including MLP and RNN. The classification performance based on the multimodal sensor system and 1D CNN exhibited the highest AUC value of 92.7%. These results suggest that our breath analyzer combined with a deep-learning algorithm can be utilized as a fast and accurate diagnostic device for lung cancer in clinical settings.

CRediT authorship contribution statement

Byeongju Lee: Conceptualization, Data curation, Formal analysis, Funding acquisition, Investigation, Methodology, Project administration, Resources, Software, Supervision, Validation, Visualization, Writing – original draft, Writing – review & editing. **Junyeong Lee:** Conceptualization, Data curation, Formal analysis, Funding acquisition, Investigation, Methodology, Project administration, Resources, Software, Supervision, Validation, Visualization, Writing – original draft, Writing – review & editing. **Jin-Oh Lee:** Conceptualization, Data curation, Formal analysis, Investigation, Methodology, Supervision, Visualization. **Yoohwa Hwang:** Conceptualization, Data curation, Formal analysis, Investigation, Methodology, Supervision. **Hyung-Keun Bahn:** Conceptualization, Data curation, Formal analysis, Investigation, Methodology. **Inkyu Park:** Investigation, Methodology, Supervision, Validation. **Sanghoon Jheon:** Conceptualization, Data curation, Formal analysis, Funding acquisition, Investigation, Methodology, Project administration, Resources, Software, Supervision, Validation, Visualization, Writing – original draft, Writing – review & editing. **Dae-Sik Lee:** Conceptualization, Data curation, Formal analysis, Funding acquisition, Investigation, Methodology, Project administration, Resources, Software, Supervision, Validation, Visualization, Writing – original draft, Writing – review & editing.

Declaration of Competing Interest

The authors declare that they have no known competing financial interests or personal relationships that could have appeared to influence the work reported in this paper.

Data Availability

The data that has been used is confidential.

Acknowledgements

B. Lee and J. Lee contributed equally to this work. This study was supported by the National Research Foundation of Korea (NRF) grant funded by the Korea government (MSIT) (No. 2021M3H4A4079271). This study was also supported by the K-Sensor Development Program (RS-2022-00154853) funded By the Ministry of Trade, Industry & Energy (MOTIE, Korea).

Appendix A. Supporting information

Supplementary data associated with this article can be found in the online version at doi:10.1016/j.snb.2024.135578.

References

[1] H. Sung, J. Ferlay, R.L. Siegel, M. Laversanne, I. Soerjomataram, A. Jemal, F. Bray, Global cancer statistics 2020: GLOBOCAN estimates of incidence and mortality worldwide for 36 cancers in 185 countries, CA Cancer J. Clin. 71 (2021) 209–249, https://doi.org/10.3322/caac.21660.

[2] S.B. Knight, P.A. Crosbie, H. Balata, J. Chudziak, T. Hussell, C. Dive, Progress and prospects of early detection in lung cancer, Open Biol. 7 (2017), https://doi.org/10.1098/rsob.170070.

[3] R. Nooreldeen, H. Bach, Current and future development in lung cancer diagnosis, Int J. Mol. Sci. 22 (2021), https://doi.org/10.3390/ijms22168661.

[4] Y. Adiguzel, H. Kulah, Breath sensors for lung cancer diagnosis, Biosens. Bioelectron. 65 (2015) 121–138, https://doi.org/10.1016/j.bios.2014.10.023.

[5] J.E. Chang, D.S. Lee, S.W. Ban, J. Oh, M.Y. Jung, S.H. Kim, S.J. Park, K. Persaud, S. Jheon, Analysis of volatile organic compounds in exhaled breath for lung cancer diagnosis using a sensor system, Sens Actuators B Chem. 255 (2018) 800–807, https://doi.org/10.1016/j.snb.2017.08.057.

[6] M.M. Hammer, S.C. Byrne, C.Y. Kong, Factors influencing the false positive rate in CT lung cancer screening, Acad. Radio. 29 (2022) S18–S22, https://doi.org/10.1016/j.acra.2020.07.040.
[7] B. Behera, R. Joshi, G.K. Anil Vishnu, S. Bhalerao, H.J. Pandya, Electronic nose: a non-invasive technology for breath analysis of diabetes and lung cancer patients, J. Breath. Res 13 (2019), https://doi.org/10.1088/1752-7163/aafc77.
[8] Y. Adiguzel, H. Kulah, Breath sensors for lung cancer diagnosis, Biosens. Bioelectron. 65 (2015) 121–138, https://doi.org/10.1016/j.bios.2014.10.023.
[9] A. Vasilescu, B. Hrinczenko, G.M. Swain, S.F. Peteu, Exhaled breath biomarker sensing, Biosens. Bioelectron. 182 (2021), https://doi.org/10.1016/j.bios.2021.113193.
[10] J. Rudnicka, T. Kowalkowski, B. Buszewski, Searching for selected VOCs in human breath samples as potential markers of lung cancer, Lung Cancer 135 (2019) 123–129, https://doi.org/10.1016/j.lungcan.2019.02.012.
[11] E. Gashimova, A. Temerdashev, V. Porkhanov, I. Polyakov, D. Perunov, A. Azaryan, E. Dmitrieva, Investigation of different approaches for exhaled breath and tumor tissue analyses to identify lung cancer biomarkers, Heliyon 6 (2020), https://doi.org/10.1016/j.heliyon.2020.e04224.
[12] B. Buszewski, T. Ligor, T. Jezierski, A. Wenda-Piesik, M. Walczak, J. Rudnicka, Identification of volatile lung cancer markers by gas chromatography-mass spectrometry: comparison with discrimination by canines, Anal. Bioanal. Chem. 404 (2012) 141–146, https://doi.org/10.1007/s00216-012-6102-8.
[13] G. Li, X. Zhu, J. Liu, S. Li, X. Liu, Metal oxide semiconductor gas sensors for lung cancer diagnosis, Chemosensors 11 (2023), https://doi.org/10.3390/chemosensors11040251.
[14] L. Liu, W. Li, Z.C. He, W. Chen, H. Liu, K. Chen, X. Pi, Detection of lung cancer with electronic nose using a novel ensemble learning framework, J. Breath. Res 15 (2021), https://doi.org/10.1088/1752-7163/abe5c9.
[15] Y. Saalberg, M. Wolff, VOC breath biomarkers in lung cancer, Clin. Chim. Acta 459 (2016) 5–9, https://doi.org/10.1016/j.cca.2016.05.013.
[16] P.J. Mazzone, X.-F. Wang, Y. Xu, T. Mekhail, M.C. Beukemann, J. Na, J.W. Kemling, K.S. Suslick, M. Sasidhar, Exhaled Breath Analysis with a Colorimetric Sensor Array for the Identification and Characterization of Lung Cancer, 2011.
[17] F. Kus, C. Altinkok, E. Zayim, S. Erdemir, C. Tasaltin, I. Gurol, Surface acoustic wave (SAW) sensor for volatile organic compounds (VOCs) detection with calix[4] arene functionalized Gold nanorods (AuNRs) and silver nanocubes (AgNCs), Sens Actuators B Chem. 330 (2021), https://doi.org/10.1016/j.snb.2020.129402.
[18] M. Castro, B. Kumar, J.F. Feller, Z. Haddi, A. Amari, B. Bouchikhi, Novel e-nose for the discrimination of volatile organic biomarkers with an array of carbon nanotubes (CNT) conductive polymer nanocomposites (CPC) sensors, Sens Actuators B Chem. 159 (2011) 213–219, https://doi.org/10.1016/j.snb.2011.06.073.
[19] R. Gasparri, M. Santonico, C. Valentini, G. Sedda, A. Borri, F. Petrella, P. Maisonneuve, G. Pennazza, A. D'Amico, C. Di Natale, R. Paolesse, L. Spaggiari, Volatile signature for the early diagnosis of lung cancer, J. Breath. Res 10 (2016), https://doi.org/10.1088/1752-7155/10/1/016007.
[20] G. Peng, E. Track, H. Haick, Detecting simulated patterns of lung cancer biomarkers by random network of single-walled carbon nanotubes coated with nonpolymeric organic materials, Nano Lett. 8 (2008) 3631–3635, https://doi.org/10.1021/nl801577u.
[21] Z. Khatoon, H. Fouad, O.Y. Alothman, M. Hashem, Z.A. Ansari, S.A. Ansari, Doped SnO2 nanomaterials for e-nose based electrochemical sensing of biomarkers of lung cancer, ACS Omega 5 (2020) 27645–27654, https://doi.org/10.1021/acsomega.0c04231.
[22] R. van de Goor, M. van Hooren, A.M. Dingemans, B. Kremer, K. Kross, Training and validating a portable electronic nose for lung cancer screening, J. Thorac. Oncol. 13 (2018) 676–681, https://doi.org/10.1016/j.jtho.2018.01.024.
[23] D. Shlomi, M. Abud, O. Liran, J. Bar, N. Gai-Mor, M. Ilouze, A. Onn, A. Ben-Nun, H. Haick, N. Peled, Detection of lung cancer and EGFR mutation by electronic nose system, J. Thorac. Oncol. 12 (2017) 1544–1551, https://doi.org/10.1016/j.jtho.2017.06.073.
[24] W. Li, H. Liu, D. Xie, Z. He, X. Pi, Lung cancer screening based on type-different sensor arrays, Sci. Rep. 7 (2017), https://doi.org/10.1038/s41598-017-02154-9.
[25] B. Liu, H. Yu, X. Zeng, D. Zhang, J. Gong, L. Tian, J. Qian, L. Zhao, S. Zhang, R. Liu, Lung cancer detection via breath by electronic nose enhanced with a sparse group feature selection approach, Sens Actuators B Chem. 339 (2021), https://doi.org/10.1016/j.snb.2021.129896.
[26] K. Chen, L. Liu, B. Nie, B. Lu, L. Fu, Z. He, W. Li, X. Pi, H. Liu, Recognizing lung cancer and stages using a self-developed electronic nose system, Comput. Biol. Med 131 (2021), https://doi.org/10.1016/j.compbiomed.2021.104294.
[27] Q. Chen, Z. Chen, D. Liu, Z. He, J. Wu, Constructing an E-nose using metal-ion-induced assembly of graphene oxide for diagnosis of lung cancer via exhaled breath, ACS Appl. Mater. Interfaces 12 (2020) 17713–17724, https://doi.org/10.1021/acsami.0c00720.
[28] International Neural Network Society., IEEE Computational Intelligence Society., The 2007 International Joint Conference on Neural Networks: IJCNN 2007 conference proceedings: August 12–17, 2007, Resaissance Orlando Resort, Orlando, Florida, USA, IEEE Xplore, 2007.
[29] V.A. Binson, M. Subramoniam, L. Mathew, Discrimination of COPD and lung cancer from controls through breath analysis using a self-developed e-nose, J. Breath. Res 15 (2021), https://doi.org/10.1088/1752-7163/ac1326.
[30] M. Tirzïte, M. Bukovskis, G. Strazda, N. Jurka, I. Taivans, Detection of lung cancer with electronic nose and logistic regression analysis, J. Breath. Res 13 (2019), https://doi.org/10.1088/1752-7163/aae1b8.
[31] S. Kiranyaz, O. Avci, O. Abdeljaber, T. Ince, M. Gabbouj, D.J. Inman, 1D convolutional neural networks and applications: a survey, Mech. Syst. Signal Process 151 (2021), https://doi.org/10.1016/j.ymssp.2020.107398.
[32] K.K. Lella, A. PJA, Automatic COVID-19 disease diagnosis using 1D convolutional neural network and augmentation with human respiratory sound based on parameters: cough, breath, and voice, AIMS Public Health 8 (2021) 240–264, https://doi.org/10.3934/publichealth.2021019.
[33] S. Lekha, M.S. Suchetha, Real-time non-invasive detection and classification of diabetes using modified convolution neural network, IEEE J. Biomed. Health Inf. 22 (2018) 1630–1636, https://doi.org/10.1109/JBHI.2017.2757510.
[34] A. Dey, Semiconductor metal oxide gas sensors: a review, Mater. Sci. Eng. B Solid State Mater. Adv. Technol. 229 (2018) 206–217, https://doi.org/10.1016/j.mseb.2017.12.036.
[35] M.A.H. Khan, M.V. Rao, Q. Li, Recent advances in electrochemical sensors for detecting toxic gases: NO2, SO2 and H2S, Sens. (Switz.) 19 (2019), https://doi.org/10.3390/s19040905.
[36] S.O. Agbroko, J. Covington, A novel, low-cost, portable PID sensor for the detection of volatile organic compounds, Sens Actuators B Chem. 275 (2018) 10–15, https://doi.org/10.1016/j.snb.2018.07.173.
[37] M. Tirzite, M. Bukovskis, G. Strazda, N. Jurka, I. Taivans, Detection of lung cancer in exhaled breath with an electronic nose using support vector machine analysis, J. Breath. Res 11 (2017), https://doi.org/10.1088/1752-7163/aa7799.

Byeongju Lee received B.S. and M.S. degrees in Mechanical Engineering from KAIST in 2020 and 2022, respectively. He is currently research assistant in the Intelligent Convengence Research Lab. at the Electronics and Telecommunications Research Institute and a Ph.D student in the Micro/Nano Transducers (MINT) research group at KAIST in mechanical Engineering department since 2022. His research activities on the development of high-performance environmental sensors, gas pattern analysis with deep learning and biomarker detection for disease diagnostics.

Junyeong Lee is currently a postdoctoral researcher in the Intelligent Convengence Research Lab. at the Electronics and Telecommunications Research Institute (ETRI), Daejeon, Rep. of Korea. He received the Ph.D. degree from Kyungpook national University (Korea) in 2021. His research interests are focused on sensor applications and AI algorithms.

Jin-Oh Lee is currently a postdoctoral researcher in the Intelligent Convengence Research Lab. at ETRI, Daejeon, Rep. of Korea. He received the Ph.D. degree from Hanyang University (Korea) in 2021. His research interests include the detection of enzyme activity using nanosensors and the identification of DNA-protein interactions using nucleic acid-based biosensors.

Yoohwa Hwang is currently a hospital director in heartwell clinic, Seoul, Rep. of Korea. She worked as an assistant professor of department of thoracic and cardiovascular surgery at Seoul National University Bundang Hospital and Seoul National University College of Medicine, Seoul, Korea. She received BS and MD degree from Ewha Womans University College of Medicine and Ph.D degree from Seoul National University Graduate School of Medicine. Her research interests are focused on cancer biology, cancer imaging techniques, prognostic markers of cancers, multimodality (multiple therapies for) treatment of cancer, and evidence-based medicine.

Hyung-Keun Bahn is currently a master's student in the Department of Medical Device Development at Seoul National University College of Medicine, Seoul, Korea. He also works as a researcher at Seoul National University Bundang Hospital. His research interests includes lung cancer screening amd medical device development.

Inkyu Park received his B.S., M.S., and Ph.D. from KAIST (1998), UIUC (2003) and UC Berkeley (2007), respectively, all in mechanical engineering. He has been with the department of mechanical engineering at KAIST since 2009 as a faculty and is currently a KAIST Chair Professor. His research interests are nanofabrication, smart sensors, nanomaterial-based sensors and flexible & wearable electronics. He has published more than 160 international journal articles (SCI indexed) and 170 international conference proceeding papers in the area of MEMS/NANO engineering. He is a recipient of IEEE NANO Best Paper Award (2010) and HP Open Innovation Research Award (2009–2012).

Sanghoon Jheon is a professor of Department of Thoracic and Cardiovascular Surgery at Seoul National University College of Medicine, Seoul, Korea. His subspeciality is lung cancer surgery performing at Seoul National University Bundang Hopspital. He is currently charging a president of Asian Society for Cardiovascular and Thoracic Surgery. His research interests include lung cancer screening, minimally invasive surgery and healthcare metaverse.

Dae-Sik Lee is currently a principal researcher in the Digital Biomedical Research Lab. at ETRI, Daejeon, Rep. of Korea. He received his Ph.D. in electronic engineering under the supervision of Duk-Dong Lee from Kyungpook National University (Korea) in 2000, and the second PhD in nanoscience and nano-engineering in the Department of Electronic and Photonic System, under the supervision of Shuichi Shoji from Waseda University (Japan), 2009. His research interests include the design and the fabrication of the sensor devices and systems.